Supplemental Information to

Ultrasensitive electrochemiluminescence Immunosensor using PtAg@ carbon nanocrystals composites as labels and carbon nanotubes-chitosan / gold nanoparticles as enhancer

Meng Zhang [a], Weijian Dai [a], Mei Yan [a], Shenguang Ge [b], Jinghua Yu [a,*], Xianrang Song[c,*], Wei Xu [a]

([a] Key Laboratory of Chemical Sensing & Analysis in Universities of Shandong (University of Jinan), Chemistry and Chemical Engineering, University of Jinan, Jinan 250022, China;

[b] Shandong Provincial Key Laboratory of Fluorine Chemistry and Chemical Materials, School of Chemistry and Chemical Engineering, University of Jinan, Jinan 250022, China;

[c] Cancer Research Center, Shandong Tumor Hospital, Jinan, Shandong Province, PR China)

* Corresponding to: Jinghua Yu E-mail: ujn.yujh@gmail.com,

Xianrang Song E-mail: sxr@vip.163.com

Fax: +86-531-82765969

1. Characterization of screen-printed carbon electrodes (SPCEs)

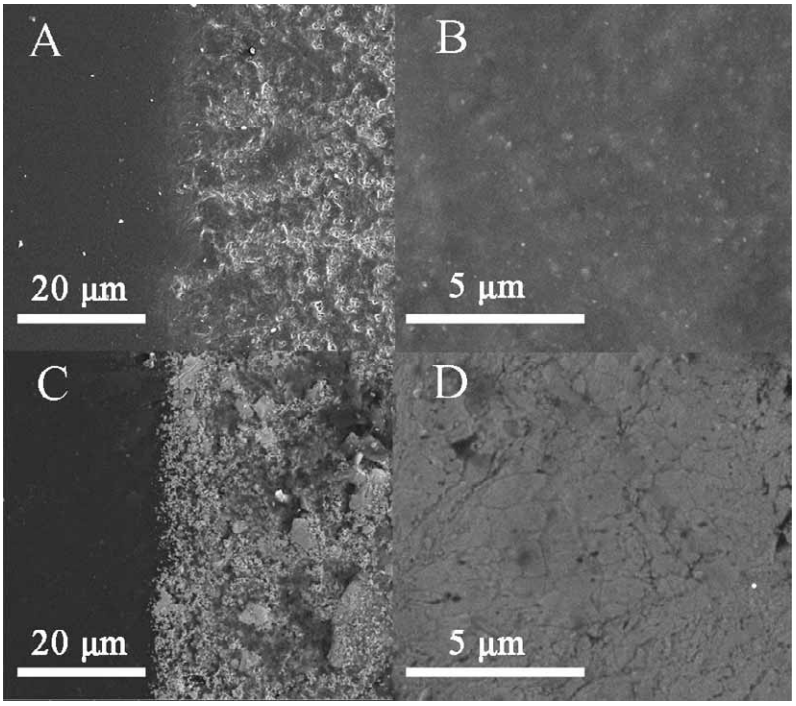

Figure S.1 Representative SEM images of SPCEs: bare CE before (A) and after polishing (B); bare RE before (C) and after polishing (D)

Screen printed electrochemical sensors provide excellent platforms for modification with a variety of nanoparticles and structurally related materials requiring no pre-treatment such as electrochemical pre-treatment via electro-deposition. The SEM images of carbon ink (CE) SPCEs and of silver/silver chloride ink (RE) were shown supplemental information, Figure S.1. The bare CE and RE without polishing were shown in Figure S.1 (A) and Figure S.1 (C), respectively. The border shows that the edge was soigne. After polishing, the smooth surface of CE and RE were obtained in Figure S.1 (B) and Figure S.1 (D), respectively.

2 The cyclic voltammograms of SPCEs

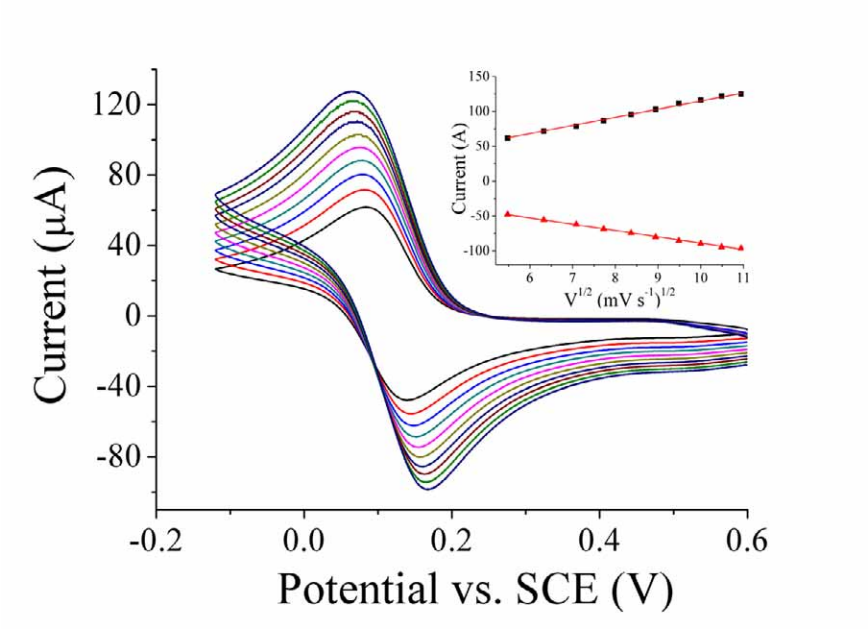

Figure S.2 Representative cyclic voltammograms of SPCEs in pH 7.4 PBS (2.5 mmol L^{-1} $Fe(CN)_6^{4-/3-}$ + 0.1 mol L^{-1} KCl, pH 7.4) at various scan rates: 30, 40, 50, 60, 70, 80, 90, 100, 110, and 120 mV s^{-1} (from inner to outer). Inset: plots of peak current vs. $v^{1/2}$.

The cyclic voltammograms of SPCEs at different scan rates were recorded in supplemental information, Figure S. 2. The peak shape of the CVs shows a relative reversible (Nernstian) electrochemical reaction, and it allows a sufficiently fast electron transfer rate for good electroanalytical performances (ΔEp= 67 mV, a value that is close to the theoretical value of 0.059 V for the redox pair) and the peak current ratio (i_{pa} / i_{pc}) is equal to 1.0. Both the anodic and cathodic peak currents increase with the square root scan rate ($v^{1/2}$) in the range between 30 and 120 mV s^{-1}. As shown in the inset of Figure S. 2, both the anodic and cathodic peak currents are linearly proportional to the square root of the scan rate increase with the square root of scan rate ($v_{1/2}$), suggesting a diffusion-limited redox process.

3 Energy dispersive spectrometer of PtAg@carbon nanocrystals

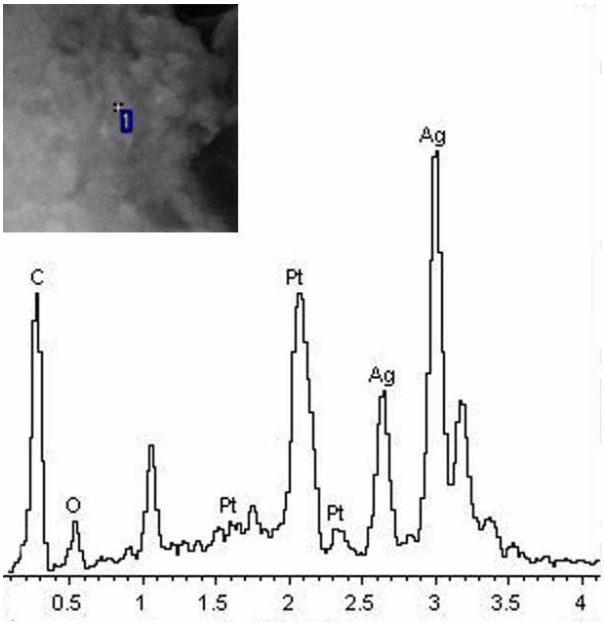

Figure S.3 Energy dispersive spectrometer of PtAg@carbon nanocrystals

The PtAg alloy conjugated with carbon nanocrystals (CNCs) was examined by using energy dispersive spectrometer (EDS) (Figure S.3). The result showed that the composition of Pt and Ag (as recorded by EDS analysis) is rich which formed bimetallic nanostructure, and we can see that CNCs could be conjugated on the surface of PtAg alloy.

4 Optimal pH

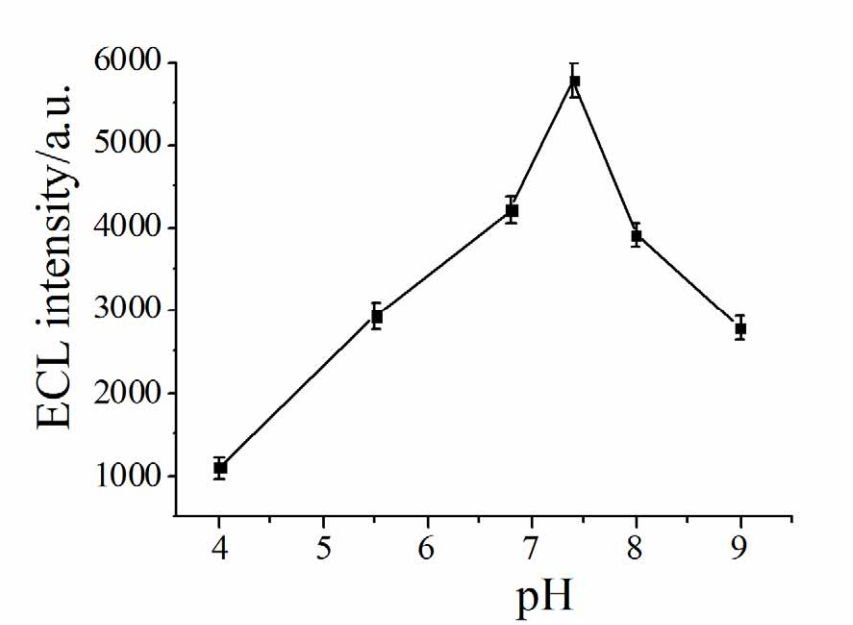

Figure S. 4 Effect of pH on ECL intensity

The pH value of substrate solution was an important factor to the ECL intensity. The ECL reaction was performed in the range from 4.0-9.0. The results showed that the optimum pH was 7.4 (Figure S.4).

5 Incubation temperature of Ab_1 and PSA

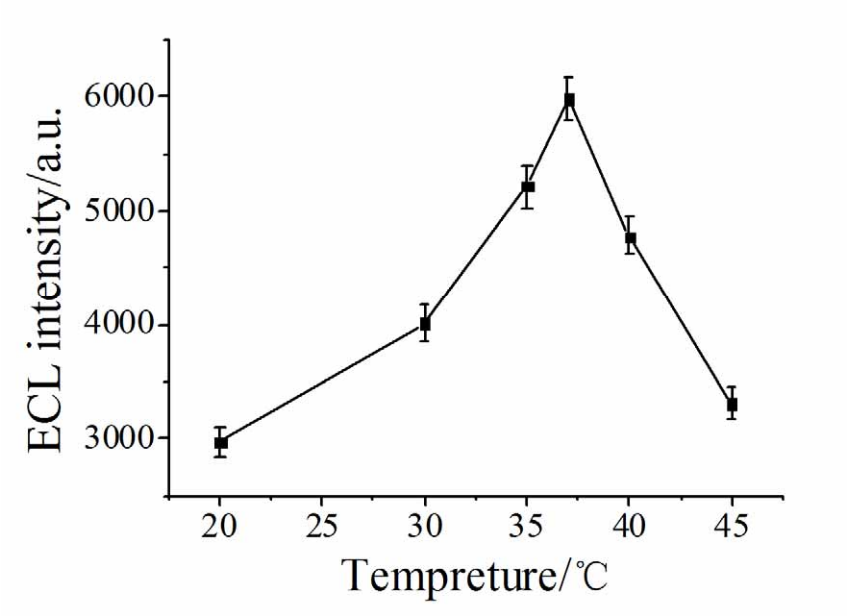

Figure S. 5 Effect of incubation temperature of Ab_1 and PSA

The effect of incubation temperature on the immunoreaction was performed. As shown in Figure S. 5, the effect of incubation temperature of Ab_1 and PSA was studied in the range from 20-45 ℃. The results showed that the ECL intensity of the immunosensor reached a maximum value at 37 ℃, indicating that the optimal incubation temperature of Ab_1 and PSA occurred at 37 ℃.

6 Incubation temperature of PSA and labeled-Ab_2

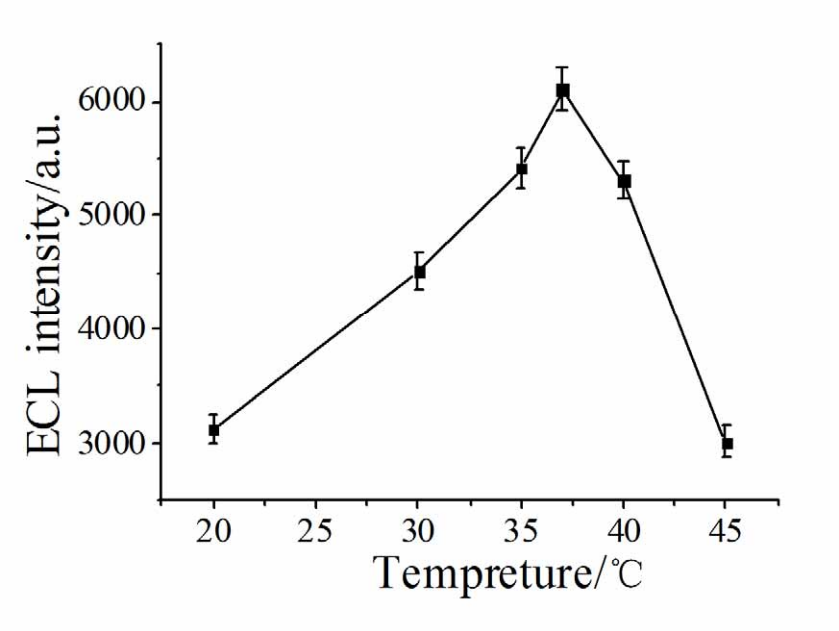

Figure S. 6 Effect of incubation temperature of PSA and labeled-Ab_2

The effect of incubation temperature on the immunoreaction was performed. As shown in Figure S. 6, the effect of incubation temperature of PSA and labeled-Ab_2 was studied in the range from 20-45 ℃. The results showed that the ECL intensity of the immunosensor reached a maximum value at 37 ℃, indicating that the optimal incubation temperature of PSA and labeled-Ab_2 occurred at 37 ℃.

7 Incubation time of Ab_1 and PSA

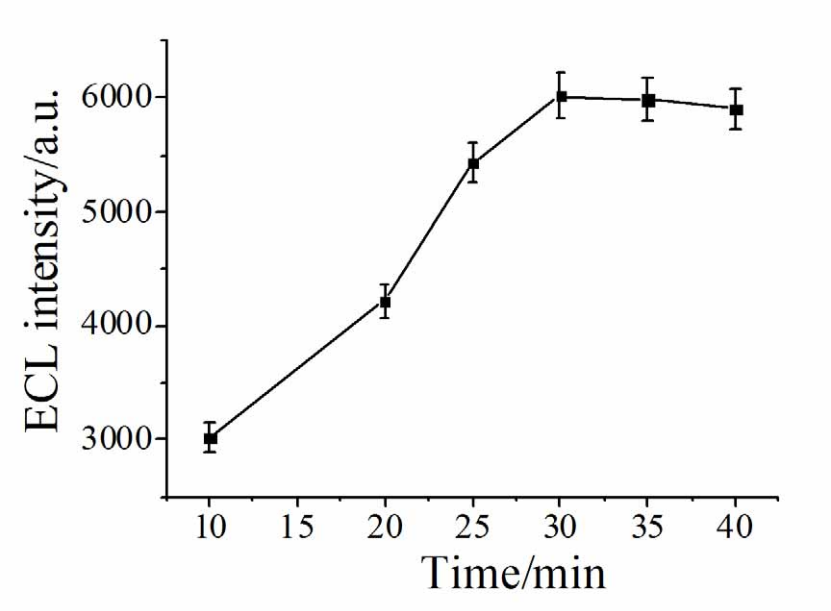

Figure S. 7 Effect of incubation time of Ab_1 and PSA

The effect of incubation time on the immunoreaction was performed. As shown in Figure S. 7, the effect of incubation time of Ab_1 and PSA was studied in the range from 10-40 min. The results showed that the ECL intensity of the immunosensor reached a maximum value in 30 min, indicating that the optimal incubation time of Ab_1 and PSA was 30 min.

8 incubation time of CEA and labeled-Ab_2

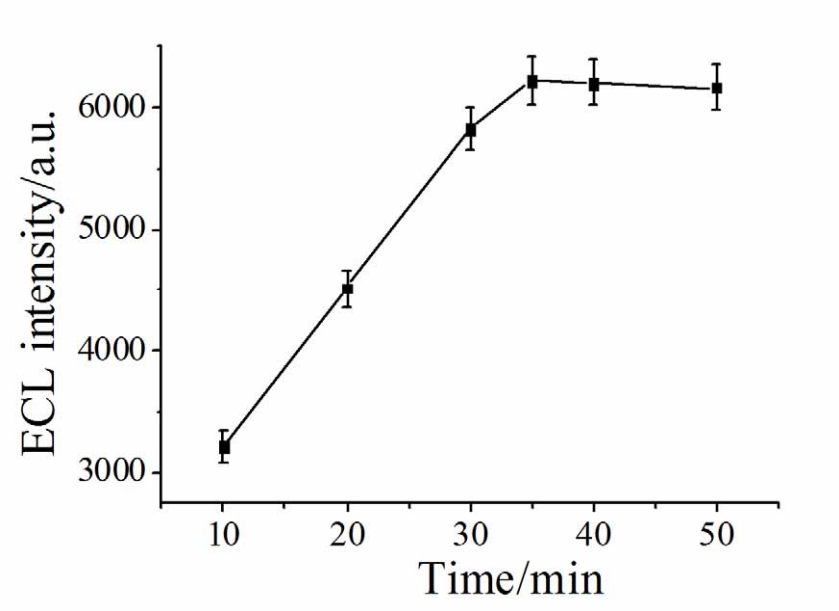

Figure S. 8 Effect of incubation time of PSA and labeled-Ab_2

The effect of incubation time of PSA and labeled-Ab_2 on the immunoreaction was studied in the range from 10-50 min. As shown in Figure S. 8, the results showed that the ECL intensity of the immunosensor reached a maximum value in 35 min, indicating that the optimal incubation time of PSA and labeled-Ab_2 was 35 min.